Overview of Planar Magnetics for High-frequency Resonant Converters*

Yue Liu, *Yufeng Song*, *Dingfan Hu*, *Yang Li*, *Zuoqian Zhang and Hongfei Wu**
(Department of Electrical Engineering,
Nanjing University of Aeronautics and Astronautics, Nanjing 211106, China)

Abstract: With the continuous development of power supplies toward miniaturization, light weights, and high levels of integration, research on high-frequency resonant conversion based on planar magnetics is becoming extensive. Combining the soft-switching characteristics of resonant converters with those of wide bandgap devices, the switching frequency can be increase to the MHz range, and the power density of the entire system can be improved considerably. However, higher switching frequencies impose new requirements for the structural design, loss distribution, and common mode (CM) noise suppression of passive magnetic components. Herein, a thorough survey of the-state-of-the-art of planar magnetics in high-frequency resonant converters is conducted. Printed circuit board winding-based planar magnetics, magnetic integration, and power-loss optimization strategies are summarized in detail. Suppression methods for CM noise in high-frequency planar magnetics are also clarified and discussed. An insight view into the future development of planar magnetics for high-frequency resonant converters is presented.

Keywords: Planar magnetics, resonant converter, matrix transformer, magnetic integration, PCB winding, loss model, loss measurement, CM noise suppression

1 Introduction

Identification of ways to achieve higher efficiency and power density has always been the main focus of research pertaining to direct current (DC)-DC converters [1-2]. Because of the excellent soft-switching performance, resonant converters, especially LLC converters, have been deployed in many applications to achieve high efficiency, high-power density, and high reliability characteristics. With the development of Gallium nitride (GaN) devices, the switching frequency of resonant converters has extended to frequencies up to (or higher than) the MHz range, thus introducing new challenges for design, optimization, integration, and fabrication of high-frequency resonant converters [3-5].

Owing to the excellent switching performance of GaN devices, active devices are no longer the main limitations of power density and efficient performance for resonant converters [6-7]. However, as the switching frequency increases, the high-frequency magnetic components, i.e., the transformer and inductor, have become the bottlenecks for the overall power density and efficiency of a resonant converter.

From the loss distribution of a high-frequency resonant converter shown in Fig. 1, it can be observed that passive magnetics, including transformers and resonant inductors, account for the highest proportion of the total loss of the entire converter. Hence, planar magnets play a significant role in the final performance of the resonant converter. To achieve higher power density and lower height, the magnetic core structure has also been developed toward planarization and integration. Likewise, the traditional Litz wire winding has gradually been replaced by printed circuit board (PCB) winding to achieve good heat dissipation, low-leakage inductance, and easy manufacturing characteristics. The improvements of the planar magnetic core and PCB winding provide more possibilities for higher efficiency and power density.

Manuscript received July 5, 2022; revised July 22, 2022; accepted July 29, 2022. Date of publication December 31, 2022; date of current version October 22, 2022.
* Corresponding Author, E-mail: wuhongfei@nuaa.edu.cn
* Supported by the National Natural Science Foundation of China (52122708, 51977105) and Natural Science Foundation of Jiangsu Province, China (BK20200017).
Digital Object Identifier: 10.23919/CJEE.2022.000039

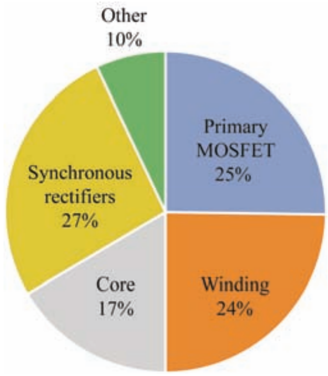

Fig. 1 Loss distribution of resonant converters

However, although planar magnetic technology in conjunction with the use of PCB windings has many of the above advantages, it also introduces some additional challenges given the use of high-frequency and planarization processes. For magnetic cores, the heights of the planar magnets tend to be much lower than common magnets. Therefore, the magnetic plates account for a larger proportion of the total magnetics. Hence, more attention should be paid to the losses and volumes of the magnetic plates that operate as nonwinding magnets. In addition, for windings, as the switching frequency increases, the effects of eddy current loss, hysteresis loss, and skin and proximity effects can also not be ignored [8-9]. Moreover, in the field of PCB winding applications, common-mode (CM) noise caused by the large interlayer capacitance is another new serious problem.

Because of the numerous complex interfering factors listed above, the design process of the planar magnetics is multidimensional and complex. To achieve higher efficiency and power density, four key technologies about the planar magnetic core and winding for high-frequency resonant converters are studied and summarized in depth in this overview, as shown in Fig. 2.

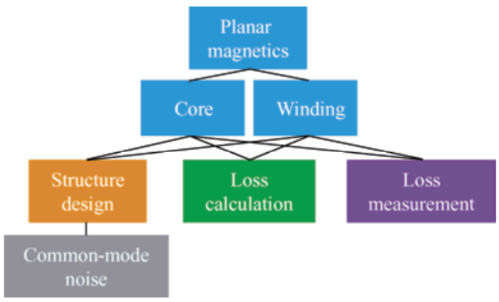

Fig. 2 Key technology of high-frequency planar magnetics

(1) Structural design: This part includes the structural design of the planar magnetic core and the configurations of PCB windings which directly determine the performance of the magnets. Meanwhile, during the structural design process, the leakage inductance, magnetizing inductance, interlayer capacitance, and other parasitic parameters should meet the restrictions of the resonant converters.

(2) Loss calculation methods: Loss is key point of the planar magnetics. The accuracy and simplicity of the loss calculation methods determine the final design results to a large extent. In the actual design process, suitable loss calculation methods should be chosen for different applications.

(3) Loss measurement methods: The accurate measurements of core and winding losses is the basis of studying all loss calculation methods, and they are also the most effective and direct methods to evaluate the magnetic performance and optimize the magnetic core structures.

(4) CM noise suppression: Following the popularization of PCB winding applications, CM noise has been introduced as a new problem. The identification of ways to suppress the CM noise without sacrificing too much volume and efficiency is a key point for higher reliability and better electromagnetic interference (EMI) performance.

2 Structural design

When the electrical parameters of the magnetics are decided, the structural design will be the most critical factor for the performance, loss, and reliability of the magnetic components of high-frequency resonant converters. It mainly includes two parts, namely, the magnetic core, and the winding structures.

2.1 Structural design of planar magnetic cores

The trend of high density and high efficiency continuously drives the development of the magnetic core structure toward planarization and integration [10]. Meanwhile, PCB windings have replaced Litz wire windings owing to their advantages of high density and uniformity, which have received increased attention [11-12]. Figs. 3a and 3b show the planar magnetic structure with PCB windings, and the traditional magnetic structure with Litz wire windings, respectively. A detailed comparison of their advantages and disadvantages is outlined in Tab. 1. Compared with conventional magnetics, the height of planar magnetics is lower. Owing to the poor thermal conductivity of the magnetic core, the planar magnetic part with low height can dissipate heat in an easier manner through the heat sink attached to the magnetic plates. Despite the disadvantages of large footprints, turns limitations, and interlayer capacitance, their advantages of consistency, manufacturability, and low cost are more essential and suitable for high-frequency applications.

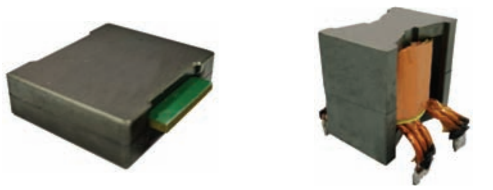

(a) Planar magnetics (b) Traditional magnetics

Fig. 3 Magnetic cores

Tab. 1 Comparison between different magnetics

Parameter	Planar magnetics (PCB windings)	Traditional magnetics (Litz wire windings)
Height	Low	High
Thermal conductivity	High	Low
Craftsmanship	High	Low
Leakage inductance	Small	Large
Footpoint	Large	Small
Turns limit	Many	Few
Interlayer capacitance	Large	Small

In the case of transformers, matrix transformers are proposed for low-voltage, and high-current output applications. The essence of the matrix transformers is the collection of multiple transformers. The primary and secondary windings of multiple submatrix transformers are connected in series or parallel, and their functions are the same as those of the centralized transformer. However, the number of PCB layers, leakage inductance, current sharing problems, and termination loss, can be improved considerably and solved by the matrix transformer structures [13].

By using the LLC resonant converter as an example, the traditional centralized transformer is shown in Fig. 4a, where S_1 and S_2 are the primary side devices, SR_1-SR_8 are the secondary side devices, and C_r, L_r, and L_m are the resonant capacitor, resonant inductor, and magnetizing inductor, respectively. As shown in Fig. 4b, the centralized transformer is divided into four matrix transformers, and the turns' ratio of each transformer is 4:1:1. The primary side is connected in series, and the secondary side is connected in parallel. Compared with the traditional centralized transformer structure, the magnetic potential between the primary and secondary windings of the matrix transformer is reduced so that the leakage inductance and winding loss are reduced. The primary windings of the four transformers are connected in series so the primary currents are equal. As a result, the secondary currents are equal. However, compared with the traditional centralized transformer, the matrix transformer will increase the overall numbers and volumes of the transformer, thus hindering further power density improvements. Hence, magnetic integration is proposed and employed to solve this problem.

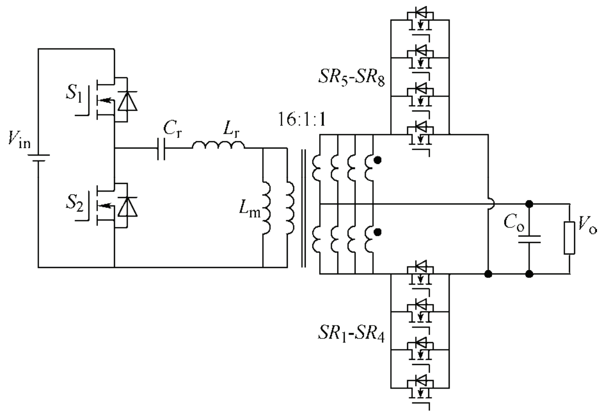

(a) Centralized transformer

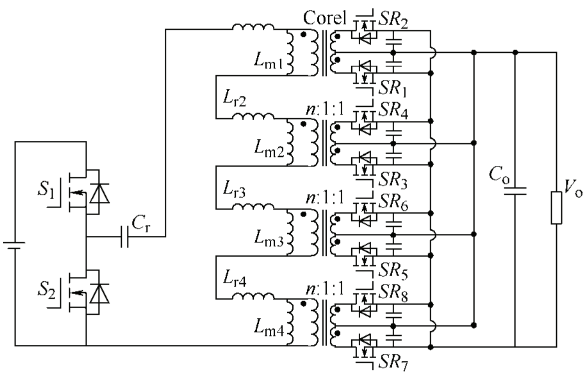

(b) Matrix transformer

Fig. 4 LLC resonant converter

As shown in Fig. 5a, the matrix transformer originally consists of four separate UI cores (Cores1-4). Further, it can be found that the magnetic flux of the nonwinding columns of two adjacent UI cores are opposite. Thus, the magnetic flux can be canceled.

Hence, the nonwinding columns can be removed, and two UI core structures can be obtained as shown in Fig. 5b (Cores1* and 2*). If the magnetic plates of two UI cores are shared and integrated, four matrix transformers can then be realized with a single magnetic core. However, there are two integration methods. The integrated structures are shown in Fig. 5c (Integrated Core1). The magnetic flux distribution of the magnetic core after integration is the same as the magnetic core before integration, and the core loss is thus almost the same as the separate core structures before integration.

However, if a UI core in the Fig. 5b is rotated by 180° and then integrated, the second magnetic integration structure shown in Fig. 5d (Integrated Core2) can be obtained, whose volume is the same as that of the first integrated structure. Nevertheless, in the magnetic plate, flux cancellation can be achieved because of the opposite direction of the magnetic flux. The flux density of the magnetic plate of the integrated Core2 is only half of that of the integrated Core1. This is helpful for high-frequency converters to achieve high efficiency, as the core loss increases substantially as switching frequency increases [14].

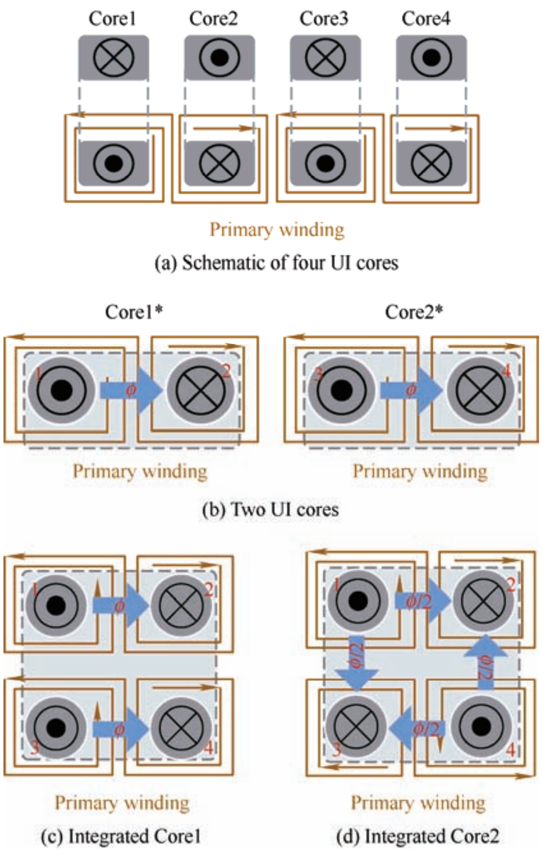

Fig. 5 Integration processes of four-matrix transformers

In addition, the integration method described above is aimed at the nonregulated DC transformer (DCX). For applications associated with a broad voltage range, a resonant inductor needs to be added into the LLC resonant converter so that the converter attains the required voltage regulation capability. As shown in Fig. 6a, Ahmed et al. [15] proposed an LLC resonant converter based on the integrated structure of a matrix transformer and an inductor. In this integrated structure, the transformer adopts a matrix magnetic structure. The resonant inductor is integrated within the transformer's core, and helps reduce core losses by expanding the equivalent cross-sectional area in the magnetic plates. However, given that the phase difference of the magnetic flux between the transformer and the resonant inductor of the LLC resonant converter is small, as shown in Fig. 6b, Liu et al. [16] proposed the configuration of the resonant inductor on the secondary side of the transformer to achieve a larger magnetic flux phase difference, and side legs without air gap were also proposed to expand the flux direction in the magnetic plate. Hence, the power density and efficiency can be increased further. However, although the side legs help extend the direction of the magnetic flux, the magnetic reluctances of the side legs will be slightly larger than those of the middle magnetic plates so that the magnetic flux distribution is uneven, and the core utilization is reduced. Therefore, Ranjram et al. [17] proposed an integrated scheme with the air gap on the magnetic plates and the side legs, which made the magnetic density distribution more uniform, but increased the number of magnets. It also led to higher costs and fixing problems. To reduce the interlayer capacitance between the PCB windings, D'Antonio et al. [18] proposed an integrated structure with controllable leakage inductance and low-winding overlap area. However, the spliced integration presented above cannot reduce further the footprints of the magnets. It was suggested in Ref. [19] to integrate the inductor column into the middle parts of the matrix transformers, as shown in Fig. 7. In addition, as shown in Fig. 8, Li et al. [20] proposed a vertical integration method of transformers and inductors based on magnetic shunts. The method can realize autonomous controllability of leakage inductance in optimal magnetizing inductance conditions, and the switching frequency range can be optimized so that high efficiency can be achieved over a broad input voltage range.

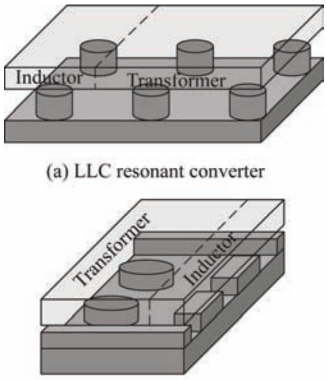

(a) LLC resonant converter

(b) CLL resonant converter

Fig. 6 Integrated cores for resonant converters

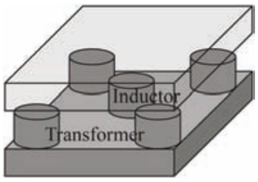

Fig. 7 Five-leg transformers with leakage

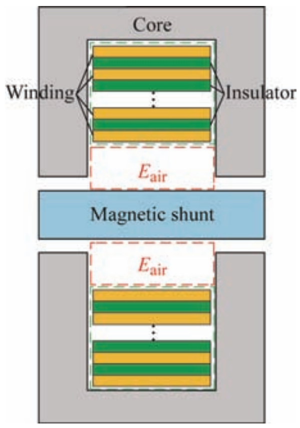

Fig. 8 Integrated structures with magnetic shunt

Further, for applications with output currents ranging from tens to hundreds of amps, the current stress of the secondary rectifiers for single-phase LLC resonant converters will be considerably high, and the conduction loss will be proportional to the square of current (which will increase substantially). In addition, given that there is only one filter capacitor of the LLC resonant converter, its output current ripple is relatively large. Therefore, as shown in Fig. 9, by increasing the phase of the LLC resonant converters, scholars have studied the three-phase interleaved parallel LLC resonant converters [21]. On this basis, for the three-phase transformer and three-phase inductance, an integration scheme is proposed as shown in Fig. 10 [22-23]. The transformer and the inductor adopt both the integrated winding and the integrated magnetic core structures.

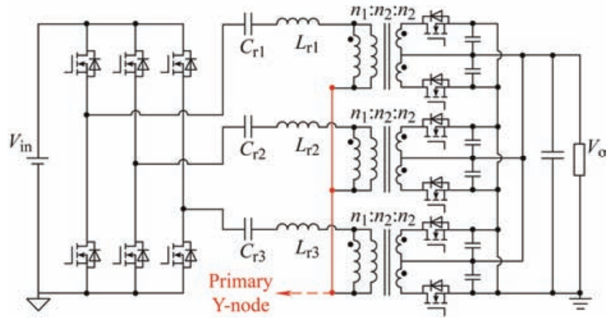

Fig. 9 Three-phase LLC resonant converters

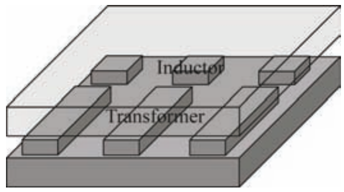

Fig. 10 Three-phase integrated cores

LLC resonant converters are favored in the field of unidirectional energy conversion. For the field of bidirectional conversion, the topology of the CLLC resonant converter is shown in Fig. 11, which can be regarded by adding an L-C series resonator on the secondary side based on the LLC converter, which makes the equivalent circuit of the CLLC converter in the forward and reverse operation completely the same, where S_1-S_4 are the primary side devices, S_5-S_8 are the secondary side devices, and L_{rp}, L_{rs}, C_{rp}, C_{rs}, and L_m form the resonant tank. However, the addition of extra resonant elements increases the overall loss and volume of the converter, which is not helpful for the improvement of the power density of the entire converter. It is feasible to integrate multiple magnets by splicing and sharing. However, as the number of magnets increases, both the structural design and the machining process become increasingly complex.

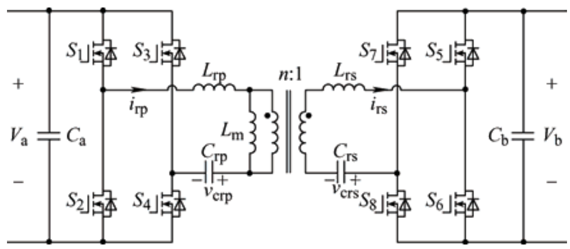

Fig. 11 CLLC resonant converter

The leakage inductance is in series with the transformer which has the same function as the resonant inductance. However, owing to the high-coupling degree of the primary and secondary windings in the planar transformer, the leakage inductance is too small to act as a resonant inductance. In addition, the use of an extra resonant inductor is equivalent to an extra volume and loss. Therefore, a method was proposed in Ref. [24] to increase the leakage inductance of the transformer. Two EI cores were used for two transformers, as shown in Fig. 12. The turns ratios for the two winding columns are 4:2 and 2:4. Both the primary and secondary windings are in series. The functions of the middle nonwinding columns are to control further the leakage inductance. The EI magnetic core structure can change the value of the magnetizing and the leakage inductances by adjusting the air gap of the side and the center columns, respectively. However, the magnetic flux of this integrated core structure is determined by both the excitation current and the load current. In this way, the magnetic column volume is still large, which is not helpful for higher power density. On this basis, as shown in Fig. 13, it was proposed by Li et al. [25] to cancel the center nonwinding columns of two EI cores, and nonair gap side legs were added at the four corners to improve the power density and efficiency of the magnetic core.

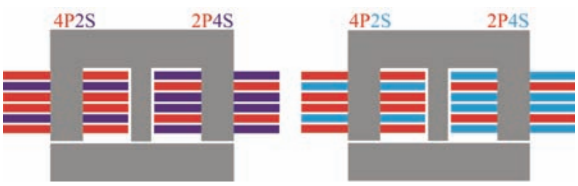

Fig. 12 Schematics of two EI cores for coupled inductors

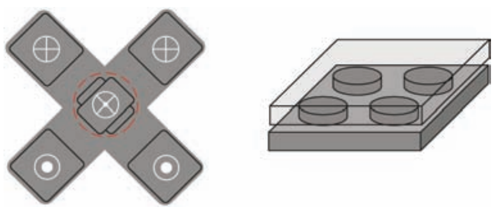

Fig. 13 Integrated cores for coupled inductors

2.2 Structural design of PCB windings

In addition to the magnetic cores, the PCB winding is the other main part of planar magnetics. Its structure is closely related to the winding loss, PCB layers, and cost. Compared with the inductor winding, the transformer winding consists of the primary winding and the secondary winding, and its complexity is improved. Therefore, the main research object of this section is the PCB winding structure of the planar transformer.

Among the various planar transformers with PCB windings, different winding arrangements have decisive influences on the winding loss. Because the magnetomotive force (MMF) distribution of the planar transformer is determined by the winding arrangement, the energy distribution of the transformer is reflected by the MMF distribution. The higher the stored energy of the transformer winding is, the greater is the leakage inductance. This means that the efficiency of the converter will be reduced if an inappropriate winding arrangement is employed [26].

As shown in Fig. 14, when the primary windings marked with ‘P’, and the secondary windings marked with ‘S’, are staggered, the peak MMF of the transformer is reduced considerably [27]. For applications with high-current outputs, it is often necessary to adopt the multiple parallel winding structure, but the staggered winding structure needs more vias and blind holes to realize the parallel connection of the windings. Meanwhile, owing to the fringing effect of the air gap, direct parallel winding structures are associated with the problem of current sharing. The current density of the winding layers close to the air gap tends to be higher. To solve these problems, as shown in Fig. 15, Yu et al. [28] proposed a segmented parallel winding structure. In other words, the distance between different parallel windings close to the air gap was equally divided, which effectively solved the problem of parallel current sharing of multilayer PCB windings.

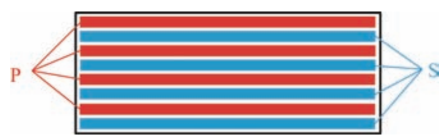

Fig. 14 Staggered winding structure

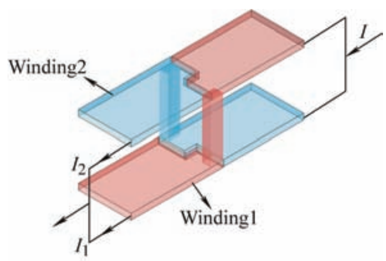

Fig. 15 Staggered parallel winding structure

In addition, it was shown [29] that the losses of different parallel or interleaved winding layers were not constant. The winding losses are related to the switching frequency. This means that different winding structures are suitable for different frequency ranges.

Recently, as the power supply voltage has become progressively smaller, the number of turns required by the transformer has also become progressively smaller. For example, for less than one turn, it is necessary to employ the fractional turn winding structure. As shown in Fig. 16, the common method used involves the winding of the magnetic columns of different areas so that the magnetic flux ratio of the primary and secondary winding turns is no longer one; in this way, half-turn, quarter-turn, and other fractional turn winding structures can be achieved [30-32]. Additionally, by winding one turn of the PCB winding on two PCB layers of the same magnetic column in parallel, half turns can be achieved as shown in Fig. 17 [33]. Likewise, by winding one turn on two magnetic columns of the same PCB layer in parallel, half turns can also be achieved, as shown in Fig. 18 [34].

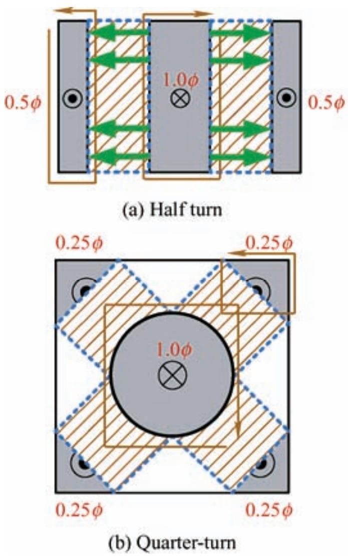

Fig. 16 Fractional turn winding

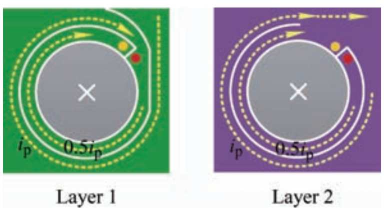

Fig. 17 Implementation of the three turns with two printed circuit board layers

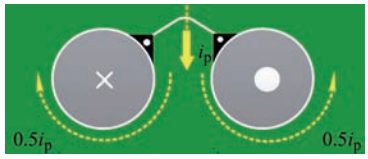

Fig. 18 Implementation of a single turn with two columns

3 Loss calculation method

During the design process of high-frequency magnetic parts, it is of great necessity to adopt the magnetic core and winding modeling to achieve the appropriate loss calculation methods. This is the basis of magnetic design because accuracy and simplicity of the calculation method affects considerably the final design results [34].

3.1 Core loss calculation method

Regarding the core loss calculation method, at present, there are two main academic directions related to this field. One relates to research conducted on the ferromagnetic properties to study the loss model and corresponding calculation formula. On this basis, optimization is conducted at different conditions. The other is based on the theory of electromagnetic fields. It is used to analyze the magnetic field distribution of the magnetic core based on finite element analysis simulation software to perform the loss calculation.

In the field of engineering applications, the experience loss model is used extensively. The core loss is usually related to the area enclosed by its hysteretic loop. Therefore, some early representative models, such as the Preisach and J-Atherton models, focused on ways to establish the accurate hysteretic loop models, but these models are only applicable to static hysteretic states [35-36]. On this basis, these models can be extended to dynamic hysteretic states by introducing some dynamic parameters [37]. However, the determination process of the correction parameters is very cumbersome and the accuracy needs to be considered. Hence, these models have many limitations for various applications. The Steinmetz equation (SE), which is fitted based on experimental data, is the most extensively used empirical formula in industry. However, the SE is only applicable to sine wave excitations [38-39]. By studying the dynamic hysteretic model, Reinert et al. [40] found that the core loss was derived from the average repeated magnetic susceptibility instead of the repeated magnetic frequency. Accordingly, the frequency term of the SE was corrected to obtain the modified Steinmetz equation (MSE), which can be applied to excitation cases induced by arbitrary waveforms. However, the low-order harmonics loss calculated by the MSE often has a large error. Meanwhile, regarding the excitation waveforms, the identification and use of a method to choose the fundamental frequency has a great influence on the final loss. To solve the above problems, the generalized Steinmetz equation (GSE) was proposed [41]. However, when the flux waveform is no longer changing monotonically, the accuracy of GSE is affected [42]. By dividing the magnetic flux waveform into those for the primary and the secondary loops, and by calculating their respective losses, the improved generalized Steinmetz equation (IGSE) [43] is obtained. Further, considering the relaxation phenomenon of the magnetic core, Muhlethaler et al. [44] obtained the new improved generalized Steinmetz equation I^2GSE.

Magnetic cores for transformers usually work with bidirectional magnetization, but those for inductors work with a DC component subject to unidirectional magnetization conditions. Brockmeyer [45] showed that the influence of a DC biased magnetic field on the inductor core loss cannot be ignored. Based on the former analysis, Mo et al. [46] introduced the calculation formula of core loss in DC bias cases. However, owing to its complex form, the formula was too complicated, and its practical value was reduced considerably [46]. Ye et al. [47] modified the SE to express more intuitively the influences of the DC biased magnetic field.

In addition, in the 1860s, the formulation of Maxwell's equations provided a theoretical basis for the study of the ferromagnetic properties of magnetic cores. According to relevant mathematical theories, the core loss can be calculated by analytical methods. Although this method has high accuracy, it requires a huge number of calculations which makes it unsuitable for complex core structures and conditions. Since the 21st century, the rapid development of computer technology made it possible for some numerical calculation methods to be applied to conduct electromagnetic calculations [48]. In recent years, well-known, commercial simulation software on the market, such as ANSOFT, ANSYS, and others, combined the finite element method with magnetic field analysis, including the hysteresis, saturation, and nonlinear characteristics of magnetic materials. The complex structures, boundary, and loss problems of the magnetic core, can now be solved by computers [49]. Up to now, although finite element analysis only considered the nonuniformity of magnetic flux distribution, and its essence is still based on some theoretical calculation models, it is still considered to be one of the most effective magnetic loss evaluation methods.

3.2 Winding loss calculation method

Winding losses constitute another major factor that is the part of total magnetic loss. At low frequencies, according to Ohm's law, the winding losses are mainly obtained by multiplying the square of the effective value of the current flowing by the DC resistance of the winding. However, as the switching frequency increases, the proximity effect and the skin effect of the current become more serious. Meanwhile, the diffused magnetic flux of the air gap will also induce extra eddy current losses. In summary, the winding loss will increase as a function of the switching frequency.

For high-frequency transformers, the calculation of the winding loss is usually based on the theoretical model of the alternating current (AC) resistance proposed by Dowell in 1966 [50]. In this model, the transformer winding on one layer is equivalent to a rectangular conductor filled in the magnetic core window; correspondingly, the AC resistance of the transformer winding can then be calculated. This method is suitable for simple copper coil windings. However, when the filling factor of the winding increases, and the switching frequency is increased further, the method's accuracy will be reduced [50]. On this basis, the famous scholar Ferreira verified the orthogonality of the high-frequency effect and the proximity effects, and then established an analytical model suitable for high-frequency windings [51-52]. However, Ferreira's method uses the Bessel function based on the eddy current of the insulated conductive cylinder subject to the action of a time-varying magnetic field, and it is accurate only when the solution object is a loose winding. Further, Nan et al.[53] used finite element simulation software to correct the Dowell's model; this achieved a significant improvement in the calculation accuracy. However, most of the correction models are based on simulation data, and thus lack a theoretical basis and general applicability prospects.

With the development of power electronic technology, the calculation methods of winding losses are becoming increasingly comprehensive. According to finite element simulations, the Center for Power Electronics Systems (CPES) of Virginia Tech in the United States, proposed a two-dimensional (2D) model of the planar winding loss [54]. According to the basic principle of electromagnetic field, the model uses a numerical calculation method to obtain the solution boundary of the 2D model to estimate the loss. Robert et al. [55] used the numerical calculation method to calculate the 2D eddy current loss by considering the skin effect of a single rectangular conductor; this process can achieve high accuracy, but it is complicated and the calculation amount is large. Therefore, it is not suitable for optimal engineering designs. Kutkut [56] adopted the segmented solution, and divided the winding loss into three stages: low, intermediate, and high frequency. The winding loss model of the planar inductor was established based on the elliptic mapping method. It has broad applicability, but the insulation distance between the winding layers is ignored, and the accuracy is reduced in multilayer PCB applications. Other researcher studies focused on the winding loss of magnets for specific topologies. Some researchers used the Fourier decomposition for the current waveform, and then obtained the winding losses at different frequencies based on the Dowell model. All the results were then added to obtain the total loss. However, the accuracies of computational methods were not considered [57-58]. Others used finite element simulation software to evaluate and optimize the final design results without using modeling directly [59].

In addition, for ultrahigh frequencies, low power, and other occasions, the air magnetic cores are extensively used owing to their extremely high-power densities. Compared with normal magnetic cores, the magnetic field of air magnetic parts is distributed completely in the air; thus, o the traditional calculation method of winding loss is no longer applicable. Lope et al. [60] proposed a semi-empirical model for the loss of the air-core inductor with multiturn windings, but at the boundary of the magnetic field, finite element simulations were still needed; this reduces the simplicity of the approach. Wang et al. [61] provided a 2D loss calculation model, but it is only applicable to air-core inductor with a single turn per layer. On this basis, for the single-layer, multiturn, air-core inductance structure, Wu et al. [62] used multiple equivalent current sources to represent the current distribution of each turn, and proposed a simulation-independent air-core inductor winding loss calculation method with the help of the table look-up method.

4 Loss measurement method

According to the third section, the loss of high-frequency magnetic components mainly includes core and winding losses. The results and performance of the final magnetic design are affected considerably by the loss calculation methods. Meanwhile, the loss measurement methods constitute the basis of the loss calculation methods, and provide verification for them to achieve iterative optimization [63-64].

4.1 Core loss measurement method

Common core loss measurement methods are mainly divided into two categories: indirect and direct. The indirect measurement methods obtain the corresponding loss value by measuring the indirect magnet parameters, such as electric, thermal, magnetic, and others, whereas the direct measurement methods directly measure the voltage and current flowing through the magnetic piece, and multiply them to obtain the final loss according to the definition of loss.

As the losses of the magnetic cores are converted to internal energy, the principle of the calorimeter method is used to calculate the loss by measuring the temperature change of the magnetic components [65-68]. The schematic of the common calorimeter method is shown in Fig. 19. The measured magnet is placed in an insulated closed container filled with the electrically insulating liquid, and the incentive source is then applied to the measured magnetic core. During the measurement process, the liquid is stirred continuously, and the loss of the magnetic parts is finally calculated according to the change of the liquid temperature. The calorimetric method has a broad range of applicability, high accuracy, and is independent of the electrical parameters of the measured magnets. However, complex calorimetric devices and a strict calibration process are required by this method to reduce errors. It is also necessary to ensure the readings, heat dissipation, and other time-consuming factors during the actual operation process. Therefore, the calorimetric method cannot be easily applied in engineering.

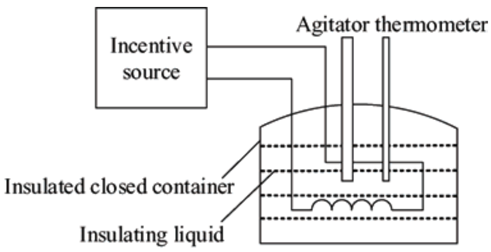

Fig. 19 Calorimetric measurements

In addition, impedance analysis allows indirect measurements of core loss. The principle is as follows: the magnetic components can be equivalent to a series model of inductance and resistance. The inductance represents the energy storage and the resistance represents the loss of the magnetic element. The equivalent resistance of the magnets at the corresponding frequency can be measured by impedance analyzers, LCR meters, and other instruments. It can then be multiplied by the square of the current flowing through the magnets to obtain the loss. However, as the output of the impedance analyzer is a small signal, it is usually necessary to amplify it through a power amplifier, and is then added to the measured magnetics. Therefore, the impedance characteristics of the magnetic component measured in the presence of large signals can be obtained, and can be substituted into the formula [69-70] to obtain the corresponding loss. The impedance analysis method is simple and easy to implement, but it is only suitable for sinusoidal excitations; additionally, its measurement accuracy will decrease as a function of frequency.

As shown in Fig. 20, the AC power meter method is a direct measurement of core loss. The principle is to record the $u(t)$ and $i(t)$ signals of the magnetic elements in one cycle, and obtain the magnetic core loss by using integration [71-72]. This method is simple to implement and has broad applicability. However, the calculated loss becomes more sensitive to phase errors at high frequencies when the impedance angle is approaching 90° [73]. To improve further this problem, scholars in the CPES at Virginia Tech reduced the impedance angle by adding a resonant capacitor to the test circuit. This can effectively reduce the influence of phase error and improve the accuracy. However, the loss of the equivalent series resistance of the resonant capacitor will also affect the measurement accuracy [74]. In addition, a double-winding air-core transformer was used to replace the resonant capacitor for the measurement of magnetic core loss in different waveform excitations. It also proposed a reactive power cancellation factor to reduce the measurement error.

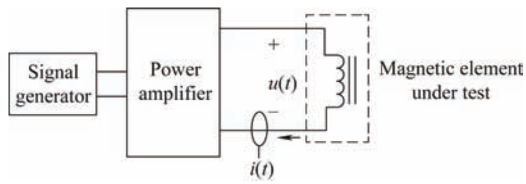

Fig. 20 Magnetic core losses attributed to alternating current (AC) measurements

To overcome the limitation of the AC power meter method in measuring the loss of high-impedance angular magnetic components, the DC power method was proposed. The principle is as follows: the required excitation voltage is provided for the measured magnetic component through the DC/AC inverter circuit, and the DC components of the input voltage and current are then measured to obtain the loss of the magnetic component. However, this method measures the input power of the entire circuit, and its error mainly arises from the inherent loss of the circuit itself.

As shown in Fig. 21, Ye et al. [75] introduced a reference magnet L_0 to measure the input powers of all the measurement devices in two different conditions. The first situation is when only the magnetic element L_0 is being measured. The second situation is when the test magnetic element L_1 is also added in the measurement. The difference of the two measurement results is the loss of the measured magnetic part. It should be noted that the equivalent inductance of the magnetics needs to be the same during the two measurements. Therefore, the $i_1(t)$ flowing in the magnet should be small enough. Therefore, only when the inductance of the measured magnet is much larger than the referenced magnet, the measurement accuracy of this method can be guaranteed.

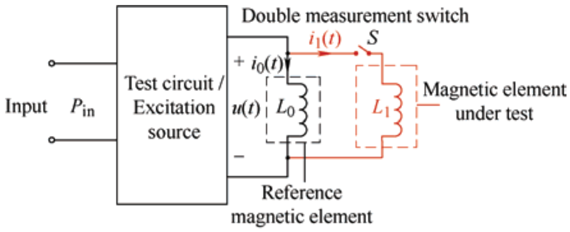

Fig. 21 Core loss test scheme based on the differential method

4.2 Winding loss measurement method

At present, there are not many research studies on the measurements of winding loss. Typically, this is obtained by the impedance method, which uses an impedance analyzer, LCR meter, and other instruments to measure the AC resistance of the winding, and measures the current of the winding, and then calculates the winding loss [76-77].

The winding loss of the magnets can also be obtained by the direct measurement method. In Ref. [78], the DC/AC inverter circuit was used to provide excitation for the magnet, and the excitation winding and the sampling winding of the measured magnets were wound in parallel. The sampling winding was then short-circuited, and the auxiliary inductor was introduced. Subsequently, excitation was applied at both ends of the magnetic component, and the winding loss was obtained by measuring the loss difference between the two cases. However, the winding loss was affected by the magnetic field. Meanwhile, owing to the influence of the inherent loss of the circuit, it is difficult to obtain accurate winding loss in real time.

Hao et al. [79] proposed a method to measure the winding loss of a planar transformer, which considered the influences of the magnetic field distribution in the magnetic core, and measured the winding loss independently. However, this method is susceptible to load resistance. Therefore, the load resistance needs to have a low inductance, and it needs to be calibrated with an impedance analyzer. However, this method can only measure the loss at a given excitation instead of a real operating condition.

To solve the above problems, Ye et al. [80] introduced the auxiliary winding, as shown in Fig. 22. The relationship of the electrical parameters of the tested and the auxiliary windings were the analyzed. As a result, the electrical parameters that only reflected the loss of the measured winding can be obtained.

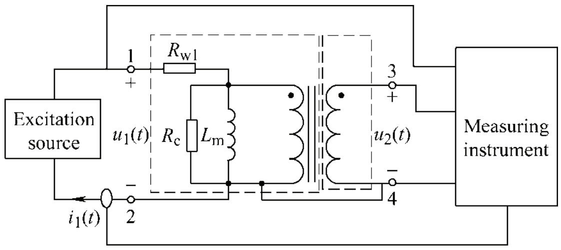

Fig. 22 Winding loss test scheme based on the AC power method

5 CM noise suppression

Although high-frequency resonant converters with planar cores and PCB windings can help achieve higher efficiency and power density, they also introduce some new problems. As the PCB winding is essentially copper foil, its interlayer winding distance is small and the facing area is large; thus, the interlayer capacitance will increase accordingly, thus resulting in high-intensity CM noise that will affect the EMI performance of the resonant converter. At present, the methods of suppressing CM noise are mainly divided into three categories, namely, impedance balance, cancellation, and shielding.

The essence of the impedance balance method is to suppress the noise from the source. The principle is to construct a new inductance or capacitance in the circuit, and form a Wheatstone bridge with the inherent reactance of the circuit. By adjusting the parameters of the additional inductance and capacitance, an electrical balanced bridge can be achieved. Thus, the CM noise is suppressed from the source of the circuit. As shown in Fig. 23, Q_1 and Q_2 are the primary power devices, SR_1 and SR_2 are the secondary synchronous rectifiers, C_{ps1}-C_{ps2} are the interlayer capacitance of the transformer. For example, it was proposed in Ref. [81] to add additional auxiliary capacitors and inductors (L_{CM}, L_{bal}, and C_{bal}) in a half bridge LLC resonant converter to achieve impedance balance, thus reducing CM noise. However, the impedance balancing method will increase the complexity and loss of the overall converter due to extra passive components.

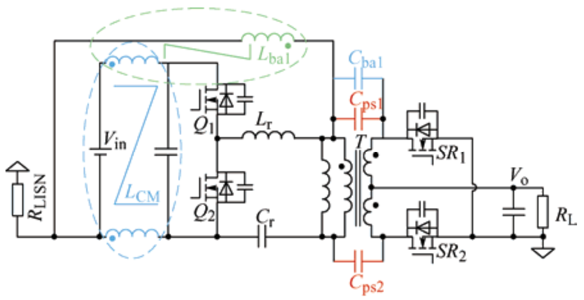

Fig. 23 Impedance balance method for LLC resonant converter

The cancellation method can be divided into transformer and topology cancellation. An additional auxiliary transformer, which is phase-staggered by 180° with the main transformer, was constructed to realize the cancellation of the CM current in Ref. [82]. However, for high-frequency applications, this scheme not only introduces additional loss, but also reduces the performance of CM noise suppression. Another suppression method is to construct a topology for CM noise cancellation. In Ref. [83], the position of one full-wave rectifier diode and the secondary winding are changed to construct a reverse CM current. In Ref. [84], two-phase, parallel LLC resonant converters are interleaved by 180° to construct the CM currents with the same magnitude and opposite directions to achieve cancellation. Han et al. [85] used the static point-structure method to replace the two primary side high-voltage devices with multiple, series-connected, low-voltage devices. Meanwhile, the switching devices within the circuit unit and between adjacent circuit units adopt complementary drive control, which also helps the effective reduction of the CM noise of the converter.

The aforementioned methods are relied on the CM noise source to reduce noise generation. In addition, CM noise can also be suppressed through the CM current conduction path. The shielding method is based on this principle [86]. As shown in Fig. 24, by inserting a shield layer, which is the same as the secondary winding, between the primary and secondary windings, and by connecting it to the static point e' of the primary side, the shield from c' to d' has the same dV/dt value as the secondary winding distributed from c to d, as shown in Fig. 25. Similarly, if the shielding layer is rotated as a whole, as shown in Fig. 26, the common current between the shielding and secondary windings is still zero. Consequently, owing to the presence of the shield, the CM current will be limited to the primary side of the transformer. However, owing to the addition of the shielding layer, the induced eddy current loss will reduce the efficiency of the converter to a certain extent. Furthermore, an additional PCB layer is required to realize the shielding layer, which also increases the cost of the resonant converter.

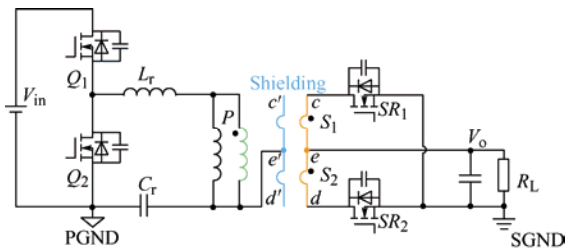

Fig. 24 LLC resonant converter with shielding

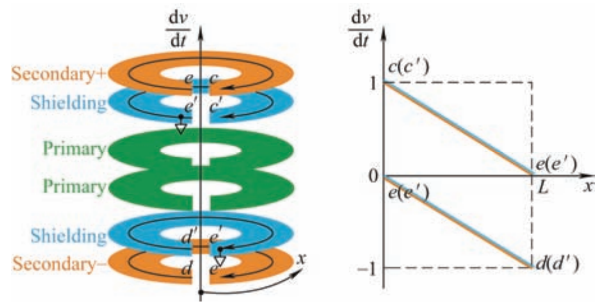

Fig. 25 Transformer structure with shielding

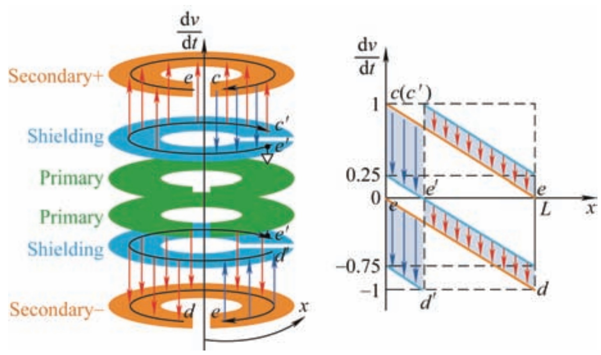

Fig. 26 Transformer structure with rotated shielding

To improve the aforementioned problems, as shown in Fig. 27, it was proposed in Ref. [87] to configure the shielding windings as part of the primary side windings. Accordingly, the winding loss can be reduced by improving the winding utilization. However, this method changes the turns' ratio of the final transformer.

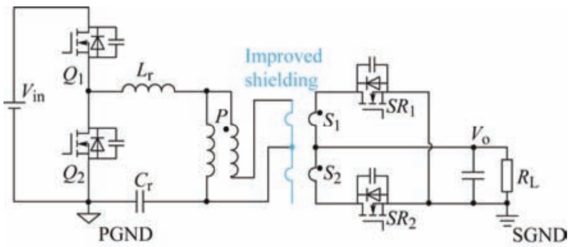

Fig. 27 LLC resonant converter with improved shielding

6 Discussion and conclusion

This study summarized the research on key technologies of high-frequency magnetic components in LLC resonant converters. The integrated structure design, loss calculation and measurement methods, and CM noise suppression methods were reviewed.

(1) High-frequency resonant converters have been extensively used in aerospace power supply systems, data-center power supplies, electric vehicle charging stations, portable consumer electronic products, and in many other fields. The magnetic components have become the bottleneck of the converter to achieve higher efficiency and higher power density.

(2) The efficiency, power density, and reliability of the magnetic components are directly determined by the magnetic core and winding structures. Planar magnetic cores with PCB windings are more attractive than traditional magnetic cores with Litz wire windings because of their consistency, manufacturability, and high-density characteristics. In addition, for specific applications, magnetic integration and specially integrated winding configurations are helpful to achieve further improvements of the overall efficiency and power density of the converter.

(3) The loss calculation methods of high-frequency magnets provide a reference for the structure design of the planar magnetics. By sorting out the existing calculation methods for magnetic cores and winding losses, it was found that the Steinmetz formula and the one-dimensional Dowell model were most commonly used. Most of the other methods are based on the above two models and only suitable for some specific occasions. In addition, with the rapid development of computer technology, theoretical calculation models combined with finite element simulations can achieve a good tradeoff between simplicity and accuracy. Hence, this method has gradually become the most common-loss calculation method.

(4) The performance evaluation of high-frequency magnetic components and the iterative optimization of the loss calculation methods were directly influenced by the loss measurement methods. Scholars have used indirect measurements, direct measurements, and other methods to evaluate core and winding losses, but these methods have some applicability, accuracy, and complexity limitations. Meanwhile, none of the loss measurement methods can realize the online measurement of core and winding losses in real working conditions, and there is also some room for further exploration.

(5) When high-frequency planar magnetics are employing PCB windings, the new problem of CM noise caused by the interlayer capacitance is unavoidable. Currently, there are two common methods for suppressing CM noise: one is to suppress the noise source, and the other is to block the conduction path. The suppression methods can be divided into three categories: impedance balance, cancellation, and shielding.

In summary, the planar magnetic technology of high-frequency resonant converters is still developing and improving, but there are still some problems that have not been solved.

(1) The integration design makes the magnetic core and winding structures more complicated. Furthermore, the influence of planarization is usually ignored.

(2) There is a lack of a universal, simple, and accurate loss calculation method.

(3) It is difficult for the existing loss measurement methods to realize online measurements in real working conditions.

References

[1] F C Lee, Q Li, A Nabih. High-frequency resonant converters: An overview on the magnetic design and control methods. *IEEE Journal of Emerging and Selected Topics in Power Electronics*, 2021, 9(1): 11-23.

[2] J D van Wyk, F C Lee. On a future for power electronics.

IEEE Journal of Emerging and Selected Topics in Power Electronics, 2021, 1(2): 59-72.

[3] B Zhao, Q Song, W Liu, et al. Overview of dual-active-bridge isolated bidirectional DC-DC converter for high-frequency-link power-conversion system. *IEEE Transactions on Power Electronics*, 2014, 29(8): 4091-4106.

[4] R C N Pilawa-Podgurski, A D Sagneri, J M Rivas, et al. Very-high-frequency resonant boost converters. *IEEE Transactions on Power Electronics*, 2009, 24(6): 1654-1665.

[5] Y Wang, O Lucia, Z Zhang, et al. A review of high frequency power converters and related technologies. *IEEE Open Journal of the Industrial Electronics Society*, 2020, 1: 247-260.

[6] K I Hwu, W C Yen, Y H Chen. Digital control of isolated two-stage DC-DC converter with synchronization considered. *2009 IEEE International Symposium on Industrial Electronics*, July 5-8, 2009, Seoul, South Korea. Piscataway: IEEE, 2009: 1598-1603.

[7] M Fu, C Fei, Y Yang, et al. A GaN-based DC-DC module for railway applications: Design consideration and high-frequency digital control. *IEEE Transactions on Industrial Electronics*, 2020, 67(2): 1638-1647.

[8] E Cardelli, L Fiorucci, E D Torre. Estimation of MnZn ferrite core losses in magnetic components at high frequency. *IEEE Transactions on Magnetics*, 2001, 37(4): 2366-2368.

[9] A Stadler, M Albach. The influence of the winding layout on the core losses and the leakage inductance in high frequency transformers. *IEEE Transactions on Magnetics*, 2006, 42(4): 735-738.

[10] M T Quirke, J J Barrett, M Hayes. Planar magnetic component technology-A review. *IEEE Transactions on Components*, 1992, 15(5): 884-892.

[11] G François, F Baudart, B Dehez. Analytical estimation of eddy current losses in PCB winding for the optimal sizing of PM slotless motor. *2019 IEEE International Electric Machines & Drives Conference (IEMDC)*, May 12-15, 2014, San Diego, CA, USA. Piscataway: IEEE, 2019: 862-869.

[12] L A R Tria, D Zhang, J E Fletcher. Planar PCB transformer model for circuit simulation. *IEEE Transactions on Magnetics*, 2016, 52(7): 1-4.

[13] D Huang, S Ji, F C Lee. LLC resonant converter with matrix transformer. *IEEE Transactions on Power Electronics*, 2014, 29(8): 4339-4347.

[14] C Fei, F C Lee, Q Li. High-efficiency high-power-density LLC converter with an integrated planar matrix transformer for high-output current applications. *IEEE Transactions on Industrial Electronics*, 2017, 64(11): 9072-9082.

[15] M H Ahmed, A Nabih, F C Lee, et al. Low-loss integrated inductor and transformer structure and application in regulated LLC converter for 48-V bus converter. *IEEE Journal of Emerging and Selected Topics in Power Electronics*, 2020, 8(1): 589-600.

[16] Y Liu, H Wu, J Zou, et al. CLL resonant converter with secondary side resonant inductor and integrated magnetics. *IEEE Transactions on Power Electronics*, 2021, 36(10): 11316-11325.

[17] M K Ranjram, D J Perreault. A 380-12 V, 1-kW, 1-MHz converter using a miniaturized split-phase, fractional-turn planar transformer. *IEEE Transactions on Power Electronics*, 2022, 37(2): 1666-1681.

[18] M D'Antonio, S Chakraborty, A Khaligh. Planar transformer with asymmetric integrated leakage inductance using horizontal air gap. *IEEE Transactions on Power Electronics*, 2021, 36(12): 14014-14028.

[19] A Nabih, Q Li, F C Lee. Magnetic integration of four-transformer matrix with high controllable leakage inductance using a five-leg magnetic. *2022 IEEE Applied Power Electronics Conference and Exposition (APEC)*, March 21-25, 2022, Phoenix, AZ, USA. Piscataway: IEEE, 2022: 693-700.

[20] M Li, Z Ouyang, M A E Andersen. High-frequency LLC resonant converter with magnetic shunt integrated planar transformer. *IEEE Transactions on Power Electronics*, 2019, 34(3): 2405-2415.

[21] E Orietti, P Mattavelli, G Spiazzi, et al. Current sharing in three-phase LLC interleaved resonant converter. *2009 IEEE Energy Conversion Congress and Exposition*, Sept. 21-24, 2009, San Jose, CA, USA. Piscataway: IEEE, 2009: 1145-1152.

[22] C Fei, R Gadelrab, Q Li, et al. High-frequency three-phase interleaved LLC resonant converter with GaN devices and integrated planar magnetics. *IEEE Journal of Emerging and Selected Topics in Power Electronics*, 2019, 7(2): 653-663.

[23] R Gadelrab, F C Lee, Q Li. Three-phase interleaved LLC resonant converter with integrated planar magnetics for telecom and server application. *2020 IEEE Applied Power Electronics Conference and Exposition (APEC)*, March 15-19, 2020, New Orleans, LA, USA. Piscataway: IEEE, 2020: 512-518.

[24] B Li, Q Li, F C Lee. High frequency PCB winding transformer with integrated inductors for a bi-directional resonant converter. *IEEE Transactions on Power*

Electronics, 2018, 34(7): 6123-6135.

[25] J Li, H Wu, W Hua, et al. Matrix inductor-transformer integration and optimization design for CLLC bidirectional resonant converter. *Proceedings of the CSEE*, 2022, 42(10): 3720-3728.

[26] K Zhang, T X Wu, J Shen, et al. Modeling and design optimization of planar power transformer for aerospace application. *Proceedings of the IEEE 2009 National Aerospace & Electronics Conference (NAECON)*, July 21-23, 2009, Dayton, OH, USA. Piscataway: IEEE, 2009: 116-120.

[27] C Ropoteanu, P Svasta, C Ionescu. A study of losses in planar transformers with different layer structure. *2017 IEEE 23rd International Symposium for Design and Technology in Electronic Packaging (SIITME)*, Oct. 27-29, 2017, Constanta, Romania. Piscataway: IEEE, 2017: 255-258.

[28] R Yu, T Chen, P Liu, et al. A 3-D winding structure for planar transformers and its applications to LLC resonant converters. *IEEE Journal of Emerging and Selected Topics in Power Electronics*, 2021, 9(5): 6232-6247.

[29] W Chen, Y Yan, Y Hu, et al. Model and design of PCB parallel winding for planar transformer. *IEEE Transactions on Magnetics*, 2003, 39(5): 3202-3204.

[30] S Li, E Rong, Q Min, et al. A half-turn transformer with symmetry magnetic flux for high-frequency-isolated DC/DC converters. *IEEE Transactions on Magnetics*, 2018, 33(8): 6467-6470.

[31] Y Liu, K Chen, C Chen, et al. Quarter-turn transformer design and optimization for high power density 1-MHz LLC resonant converter. *IEEE Trans. Ind. Electron.*, 2020, 67(2): 1580-1591.

[32] S Wang, H Wu, F C Lee, et al. Integrated matrix transformer with optimized PCB winding for high-efficiency high-power-density LLC resonant converter. *2019 IEEE Energy Conversion Congress and Exposition (ECCE)*, September 29-October 3, 2019, Baltimore, MD, USA. Piscataway: IEEE, 2019: 6621-6627.

[33] Y Jin, W Xie, N Yang, et al. High efficiency resonant DC/DC converter based on GaN device and planar transformer. *2020 IEEE 5th Information Technology and Mechatronics Engineering Conference (ITOEC)*, June 12-14, 2020, Chongqing, China. Piscataway: IEEE, 2020: 358-362.

[34] P R Wilson, J N Ross, A D Brown. Modeling frequency-dependent losses in ferrite cores. *IEEE Transactions on Magnetics*, 2004, 40(3): 1537-1541.

[35] I D Mayergoyz, G Friedman. Generalized Preisach model of hysteresis. *IEEE Trans. on Magnetics*, 1988, 24(1): 212-217.

[36] D C Jiles, D L Atherton. Theory of ferromagnetic hysteresis. *Journal of Magnetism and Magnetic Materials*, 1986, 61: 48-60.

[37] D Lin, P Zhou, W N Fu, et al. A dynamic core loss model for soft ferromagnetic and power ferrite materials in transient finite element analysis. *IEEE Transactions on Magnetics*, 2004, 40(2): 1318-1321.

[38] C P Steinmetz. On the law of hysteresis. *Transactions of the American Institute of Electrical Engineers*, 1892, 9(1): 1-64.

[39] J E Brittain. A Steinmemtz contribution to the AC power revolution. *Proceedings of the IEEE*, 1984, 72(2): 196-197.

[40] J Reinert, A Brockmeyer, R W A A De Doncker. Calculation of losses in ferro- and ferrimagnetic materials based on the modified Steinmetz equation. *IEEE Transactions on Industry Applications*, 2001, 37(4): 1055-1061.

[41] J Li, T Abdallah, C R Sullivan. Improved calculation of core loss with nonsinusoidal waveforms. *Conference Record of the 2001 IEEE Industry Applications Conference (Cat. No.01CH37248)*, Sept. 30-Oct. 4, 2001, Chicago, IL, USA. Piscataway: IEEE, 2002: 2203-2210.

[42] J Liu, T G Wilson, R C Wong, et al. A method for inductor core loss estimation in power factor correction applications. *APEC. Seventeenth Annual IEEE Applied Power Electronics Conference and Exposition (Cat. No.02CH37335)*, March 10-14, 2002, Dallas, TX, USA. Piscataway: IEEE, 2002: 439-445.

[43] K Venkatachalam, C R Sullivan, T Abdallah, et al. Accurate prediction of ferrite core loss with nonsinusoidal waveforms using only Steinmetz parameters. *2002 IEEE Workshop on Computers in Power Electronics, 2002. Proceedings.*, June 3-4, 2002, Mayaguez, PR, USA. Piscataway: IEEE, 2002: 36-41.

[44] J Muhlethaler, J Biela, J W Kolar, et al. Improved core-loss calculation for magnetic components employed in power electronic systems. *IEEE Transactions on Power Electronics*, 2012, 27(2): 964-973.

[45] A Brockmeyer. Experimental evaluation of the influence of DC-premagnetization on the properties of power electronic ferrites. *Proceedings of Applied Power Electronics Conference. APEC'96*, March 3-7, 1996, San Jose, CA, USA. Piscataway: IEEE, 2002: 454-460.

[46] W K Mo, D K W Cheng, Y S Lee. Simple approximations of the DC flux influence on the core loss power electronic ferrites and their use in design of magnetic components.

IEEE Transactions on Industrial Electronics, 1997, 44(12): 788-799.

[47] J Ye, W Chen, J Wang. Research on the core loss model under PWM wave and DC bias excitations. *Proceedings of the CSEE*, 2015, 35(10): 2601-2606.

[48] E Dlala. Comparison of models for estimating magnetic core losses in electrical machines using the finite-element method. *IEEE Trans. Magn*, 2009, 45(2): 716-725.

[49] A Rakotomatala, N Burais, P Auriol. A 2D semi-analytical method for the calculation of eddy current losses in transformer and inductance coils. *1994 Fifth International Conference on Power Electronics and Variable-Speed Drives*, Oct. 26-28, 1994, Mayaguez, London, UK. Hertford: IET, 1994: 188-191.

[50] P L Dowell. Effects of eddy currents in transformer windings. *Proceedings of the Institution of Electrical Engineers*, 1966, 113(8): 1387-1394.

[51] J A Ferreira. Improved analytical modeling of conductive losses in magnetic components. *IEEE Transactions on Power Electronics*, 1994, 9(1): 127-131.

[52] J A Ferreira. Appropriate modelling of conductive losses in the design of magnetic components. *21st Annual IEEE Conference on Power Electronics Specialists*, 1990, San Antonio, TX, USA. Piscataway: IEEE, 2002: 780-785.

[53] X Nan, C R Sullivan. An improved calculation of proximity-effect loss in high-frequency windings of round conductors. *IEEE 34th Annual Conference on Power Electronics Specialist*, *2003. PESC'03.*, June 15-19, 2003, Acapulco, Mexico. Piscataway: IEEE, 2003: 853-860.

[54] A W Lotfi, F C Lee. Two dimensional field solutions for high frequency transformer windings. *Proceedings of IEEE Power Electronics Specialist Conference–PESC'93,* June 20-24, 1993, Seattle, WA, USA. Piscataway: IEEE, 2002: 1098-1104.

[55] F Robert, P Mathys, J P Schauwers. A closed-form formula for 2-D ohmic losses calculation in SMPS transformer foils. *IEEE Transactions on Power Electronics*, 2001, 16(3): 437-444.

[56] N H Kutkut. A simple technique to evaluate winding losses including two-dimensional edge effects. *Proceedings of APEC 97-Applied Power Electronics Conference*, Feb. 27-27, 1997, Atlanta, GA, USA. Piscataway: IEEE, 2002: 368-374.

[57] K V Iyer, W P Robbins, K Basu, et al. Transformer winding losses with round conductors for duty-cycle regulated square waves. *2014 International Power Electronics Conference (IPEC-Hiroshima 2014 - ECCE ASIA)*, May 18-21, 2014, Hiroshima, Japan. Piscataway: IEEE, 2014: 3061-3066.

[58] W Yuan, X Huang, P Meng, et al. An improved winding loss analytical model of Flyback transformer. *2010 Twenty-Fifth Annual IEEE Applied Power Electronics Conference and Exposition (APEC)*, Feb. 21-25, 2010, Palm Springs, CA, USA. Piscataway: IEEE, 2010: 433-438.

[59] M Cui, X You, Y Li, et al. Planar transformer design in GaN based LLC resonant converter. *2014 International Power Electronics and Application Conference and Exposition*, Nov. 5-8, 2014, Shanghai, China. Piscataway: IEEE, 2014: 1353-1357.

[60] I Lope, C Carretero, J Acero, et al. AC power losses model for planar windings with rectangular cross-sectional conductors. *IEEE Transactions on Power Electronics*, 2014, 29(1): 23-28.

[61] X Wang, L Wang, L Mao, et al. Improved analytical calculation of high frequency winding losses in planar inductors. *IEEE 2018 Energy Conversion Congress and Expo*, Sept. 23-27, 2018, Portland, OR, USA. Piscataway: IEEE, 2018: 4336-4340.

[62] M Wu, L Wang, D Ahmed, et al. An accurate analytical model to evaluate the winding loss of a single-layer multi-turn planar air-core PCB-inductor. *2021 IEEE Energy Conversion Congress and Exposition (ECCE)*, Oct. 10-14, 2021, Vancouver, BC, Canada. Piscataway: IEEE, 2021: 5483-5487.

[63] P Marketos, J P Hall, S E Zirka. Power loss measurement and prediction of soft magnetic powder composites magnetized under sinusoidal and nonsinusoidal excitation. *IEEE Transactions on Magnetics*, 2008, 44(11): 3847-3850.

[64] J Ye, W Chen, J He. A differential method of high-frequency magnetics core loss test scheme. *2014 IEEE 5th International Symposium on Power Electronics for Distributed Generation Systems (PEDG)*, June 24-27, 2014, Galway. Piscataway: IEEE, 2014: 1-5.

[65] J Wang，W Chen. Study of calorimetric method to measure loss of super low loss angle core. *Advanced Technology of Electrical Engineering and Energy*, 2012, 31(4): 6-9.

[66] P Gradzki. Core loss characterization and design optimization of high-frequency power ferrite devices in power electronics applications. Blacksburg: Virginia Polytechnic Institute and State University, 1992.

[67] F D Tan, J L Vollin, S M Cuk. A practical approach for magnetic core-loss characterization. *IEEE Transactions on Power Electronics*, 1995, 10(2): 124-130.

[68] D R Turner, K J Binns, B N Shamsaddeen, et al. Accurate measurement of induction motor losses using balance

calorimete. *Electric Power Applications*, 1991, 138(5): 233-242.

[69] J Zhang, G Skutt, F C Lee. Some practical issues related to core loss measurement using impedance analyzer approach. *Proceedings of IEEE Applied Power Electronics Conference*, March 5-9, 1995, Hyatt Regency, Dallas, USA. Piscataway: IEEE, 1995: 547-553.

[70] G R Skut, F C Lee. Some practical issues related to core loss measurement using impedance analyzer. *Proceedings of 1995 IEEE Applied Power Electronics Conference and Exposition - APEC'95*, March 5-9, 1995, Dallas, TX, USA. Piscataway: IEEE, 1995: 547-554.

[71] D Y Chen. High-frequency core loss characteristics of amorphous magnetic alloy. *Proceedings of the IEEE*, 1981, 69(7): 853-855.

[72] M S Lancarotte, C Goldemberg, A D A Penteado. Estimation of FeSi core losses under PWM or DC bias ripple voltage excitations. *IEEE Transactions on Energy Conversion*, 2005, 20(2): 367-372.

[73] C Yan，J He，X Guo. Influence of different excitation waveforms on ferrite core loss. *Journal of Magnetic Materials and Devices*, 2011, 42(2): 37-42.

[74] D Hou, M Mu, F C Lee, et al. New high-frequency core loss measurement method with partial cancellation concept. *IEEE Transactions on Power Electronics*, 2017, 32(4): 2987-2994.

[75] J Ye, W Chen. The method and device based on the differential power for measurement of high-frequency core losses. *Proceedings of the CSEE*, 2017, 37(16): 4834-4841, 4909.

[76] C R Sullivan. Computationally efficient winding loss calculation with multiple windings, arbitrary waveforms, and two-dimensional or three-dimensional field geometry. *IEEE Trans. on Power Electronics*, 2001, 16(1): 142-150.

[77] J Ye, W Chen. A novel evaluation and test method for gapped magnetics high-frequency winding losses. *Proceedings of the CSEE*, 2015, 35(7): 1749-1755.

[78] J Wang, W Chen. Deduction of copper loss from core loss under square wave excitation. *Journal of Nanchang University*, 2012, 34(3): 279-282.

[79] Y Hao, W Eberle, Y Liu. A practical copper loss measurement method for the planar transformer in high-frequency switching converters. *IEEE Transactions on Industrial Electronics*, 2007, 54(4): 2276-2287.

[80] J Ye, W Chen, R Zheng, et al. The direct measurement method of magnetic winding losses. *Proceedings of the CSEE*, 2018, 38(5): 1369-1374.

[81] D Fu, S Wang, P Kong, et al. Novel techniques to suppress the common-mode EMI noise caused by transformer parasitic capacitances in DC-DC converters. *IEEE Transactions on Industrial Electronics*, 2013, 60(11): 4968-4977.

[82] Y P Chan, B M H Pong, N K Poon, et al. Common-mode noise cancellation by an antiphase winding in multilayer isolated planar transformer. *IEEE Transactions on Electromagnetic Compatibility*, 2014, 56(1): 67-73.

[83] S Zhang, X Wu. Analysis and suppression of conducted EMI emissions for front-end LLC resonant DC/DC converters. *IEEE Transactions on Power Electronics*, 2019, 34(2): 1032-1037.

[84] D Fu, P Kong, S Wang, et al. Some practical issues related to core loss measurement using impedance analyzer approach. *2008 IEEE Power Electronics Specialists Conference*, June 15-19, 2008, Rhodes, Greece. Piscataway: IEEE, 2008: 1144-1150.

[85] Y Han, G Li, H Shi, et al. Analysis and suppression of common-mode EMI noise in 1 MHz 380 V-12 V DCX converter with low NFoM devices. *IEEE Transactions on Power Electronics*, 2021, 36(7): 7903-7931.

[86] Y Yang, D Huang, F C Lee, et al. Analysis and reduction of common mode EMI noise for resonant converters. *2014 IEEE Applied Power Electronics Conference and Exposition - APEC 2014*, March 16-20, 2014, Fort Worth, TX, USA. Piscataway: IEEE, 2014: 566-571.

[87] C Fei, Y Yang, Q Li, et al. Shielding technique for planar matrix transformers to suppress common-mode EMI noise and improve efficiency. *IEEE Transactions on Industrial Electronics*, 2018, 65(2): 1263-1272.

Yue Liu was born in Jiangsu Province, China, in 1997. He received the B.S. degree in Electrical Engineering from Nanjing University of Aeronautics and Astronautics (NUAA), Nanjing, China, in 2019, where he is currently working toward the Ph.D. degree in Electrical Engineering. His main research interests include magnetic integration and resonant converters.

Yufeng Song was born in Jiangsu Province, China, in 1999. He is currently working toward the B.S. degree in Electrical Engineering from Nanjing University of Aeronautics and Astronautics (NUAA), Nanjing, China. His main research interests include magnetic integration and resonant converters.

Dingfan Hu was born in Zhejiang Province, China, in 2000. He is currently working toward the B.S. degree in Electrical Engineering from Nanjing University of Aeronautics and Astronautics (NUAA), Nanjing, China. His main research interests include magnetic integration and resonant converters.

Yang Li was born in Jiangsu Province, China, in 2000. She is currently working toward the B.S. degree in Electrical Engineering from Nanjing University of Aeronautics and Astronautics (NUAA), Nanjing, China. Her main research interests include magnetic integration and resonant converters.

Zuoqian Zhang was born in Jiangxi Province, China, in 1997. He received the B.S. degree in Electrical Engineering from Nanjing University of Aeronautics and Astronautics (NUAA), Nanjing, China, in 2020, where he is currently working toward the Ph.D. degree in Electrical Engineering. His main research interests include DC-DC converters and control.

Hongfei Wu (S'11-M'13-SM'18) received the B.S. and Ph. D degrees in Electrical Engineering and Power Electronics and Power Drives from Nanjing University of Aeronautics and Astronautics (NUAA), Nanjing, China, in 2008 and 2013, respectively.

Since 2013, he has been with the Faculty of Electrical Engineering, NUAA, and is currently a Professor with College of Automation Engineering, NUAA. He has authored and co-authored more than 170 peer-reviewed papers published in journals and conference proceedings. He is the holder of more than 40 patents. His research interests are high performance power converters, wide-band-gap devices applications and magnetic integration.

Dr. Wu was the recipient of the Best Associate Editor of Journal of Power Electronics (2018), the Outstanding Reviewer of IEEE Transactions on Power Electronics (2013), the Changkong Scholar Award and Young Scholar Innovation Award of NUAA (2017). He serves as an Associate Editor of Journal of Power Electronics, CPSS Transactions on Power Electronics and Applications, Chinese Journal of Electrical Engineering and Power Electronic Devices and Components. He is a Gest Associate Editor of IEEE Journal of Emerging and Selected Topics in Power Electronics.